Mimicking surface plasmons in acoustics at low frequency

Li Quan,[1,2] Feng Qian,[1,3] Xiaozhou Liu,[1,*] Xiufen Gong,[1] and Paul A. Johnson[4]

[1]*Key Laboratory of Modern Acoustics, Ministry of Education, Institute of Acoustics and School of Physics, Collaborative Innovation Center of Advanced Microstructures, Nanjing University, Nanjing 210093, People's Republic of China*

[2]*Department of Electrical and Computer Engineering, The University of Texas at Austin, Austin, Texas 78713, USA*

[3]*College of Physics and Electronic Engineering, Changshu Institute of Technology, Changshu 215500, People's Republic of China*

[4]*Geophysics Group EES-17, Los Alamos National Laboratory, Los Alamos, New Mexico 87545, USA*

(Received 20 August 2014; published 14 September 2015)

Extraordinary optical transmissions through metallic films with arrays of subwavelength holes have attracted much attention in the past few years, and surface plasmons are accepted as the key factor in their origin. Further studies showed that the abilities of surface plasmons can also be extended to achieve light collimation. Here, we show that collective surface oscillation can also occur in acoustics, and different from previous reports, we demonstrate that extraordinary acoustic transmissions and sound collimation can be achieved when the wavelength is much longer than the characteristic length of the sample. The excitation and detection approaches of the acoustic surface oscillation are also presented. Our findings should open up prospects for acoustic applications, and many exotic optical phenomena related to surface plasmons can be anticipated with their counterparts in acoustics.

DOI: 10.1103/PhysRevB.92.104105 PACS number(s): 43.20.+g, 43.35.+d, 46.40.Cd

I. INTRODUCTION

Surface plasmons (SPs) are the coherent electron oscillations that exist at the interface between two materials, where the real part of the dielectric function changes sign across the interface. First predicted by Ritchie [1], SPs have been studied for almost 60 years. SPs are of interest to scientists in multiple fields, ranging from physicists, chemists, and materials scientists to biologists due to their unique properties and potential applications in many fields, such as electromagnetic wave manipulation [2,3], particles or cell trapping and transport [4–7], molecular detection [8,9], and biological sensing [10]. It is reported that SPs can result in Raman signal enhancement [11,12], extraordinary optical transmission [13,14], light beaming [15], SP lasers [16,17], nondiffracting SP beams [18,19], quantum plasmonics [20], and acoustoplasmonic control [21], showing the unlimited potential and wide application of SPs. Among all the progress related to SPs, the discoveries of extraordinary optical transmission [13,14] and light collimation [15] stand out as the notable landmarks in the progress of the research of SPs. Although SPs are accepted as one of the most important factors in the physical origins of extraordinary optical transmissions and light collimation, there are still debates on whether the SPs play a positive or a negative role on extraordinary optical transmission [22,23]. However, all of the exotic phenomena and wide applications proposed above are unique to electromagnetic waves. Acoustic waves, as a more common wave phenomenon in nature, do not support these properties due to the lack of collective surface oscillations in acoustics.

By analogy, extraordinary acoustic transmission phenomena have been reported recently [24–27], but their origin is attributed to either Fabry-Perot resonance in the slits or coherent diffraction induced by the periodicity [28–31]. The possibility of using excitation of structure-induced acoustic surface waves in a perfectly rigid body to achieve sound collimation has also been discussed [32–35]. Theory studies show that the dispersion curves of the surface waves caused by the grooves' structure is similar to the SP dispersion relationship [34]; then the spoof surface acoustic waves induced by the grooves' structure were used to realize acoustic imaging and focusing [36,37]. Although there are a lot of reports about extraordinary acoustic transmission and sound collimation realized by acoustic gratings' and grooves' structures, all these phenomena were achieved when the wavelengths were near the period of the structures [24–35]. This is because compared with the periodicity of the structure, the relatively low weight of these acoustic surface waves cannot affect extraordinary acoustic transmission and sound collimation when the wavelength is much longer than the period of the decorated structures [33], which limits the miniaturization of acoustic devices in practical applications. How to achieve these phenomena when the wavelength is much larger than the period of the structure remains unanswered.

In this paper, we present the realization of extraordinary acoustic transmission and sound collimation when the wavelength is much longer than the period length of the sample. The samples, based on decorated periodical Helmholtz resonators (HRs) on the output side of hard plates, strongly couple the incident wave into acoustic surface waves that mimic SPs. The HRs, behaving like free electrons in the metallic surface, oscillate collectively on the surface of the plate. These imitation SPs, readily controllable on all length scales in order to design with almost arbitrary dispersion, significantly enhance the transmission efficiency and improve the collimation effect.

II. EXTRAORDINARY ACOUSTIC TRANSMISSION

A rectangular acoustic grating with very narrow apertures is shown in Fig. 1(a). Different from the acoustic grating reported in Ref. [26], we decorated four HRs on each of the rectangular body. The thickness of the grating was 10 mm. The width of the aperture was 1 mm. The period of the HRs was 6 mm. The

*xzliu@nju.edu.cn

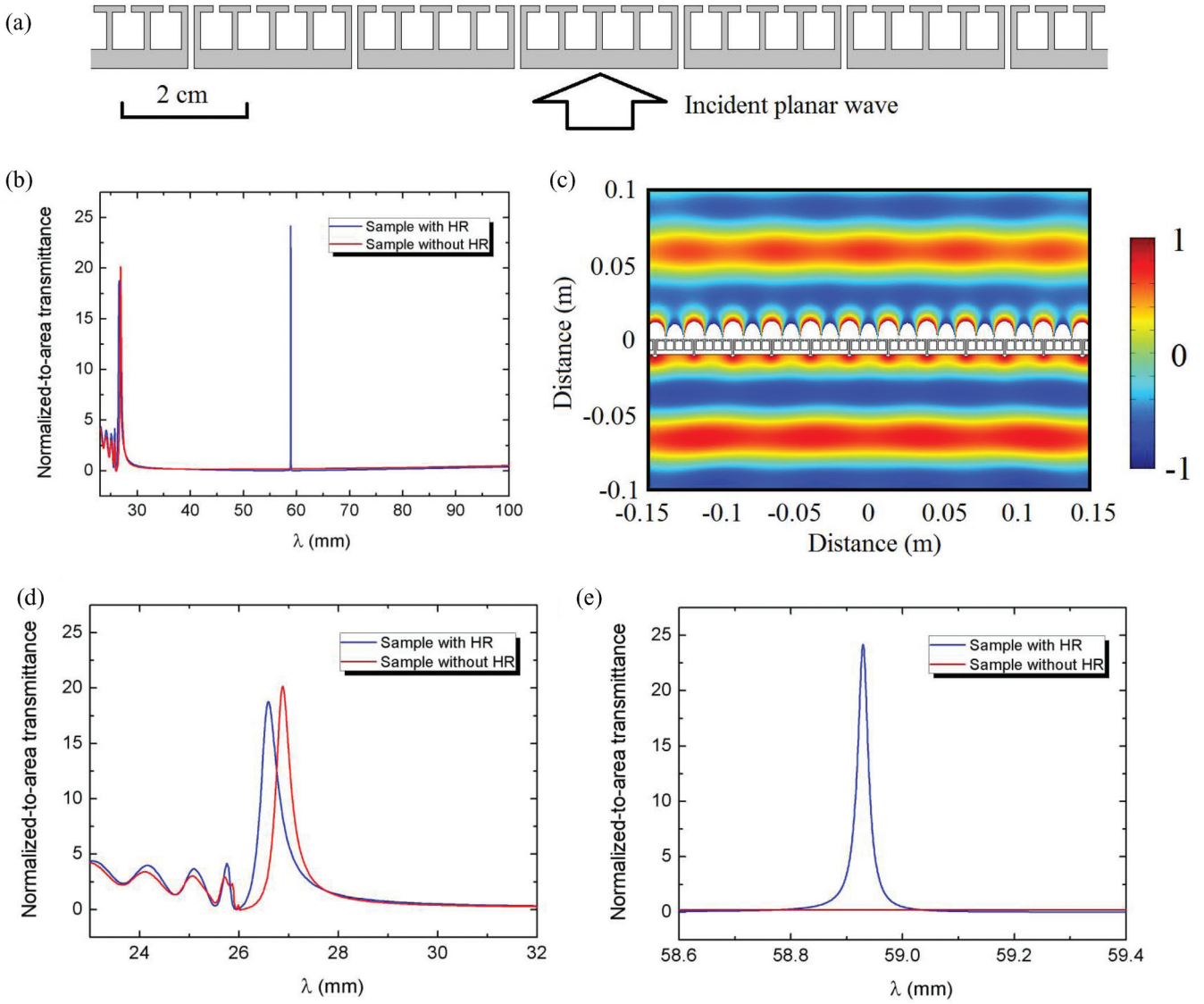

FIG. 1. (Color) (a) Schematic diagram of the structure to realize extraordinary acoustic transmission. The structure is an acoustic grating decorated with four HRs on each rectangular body. (b) Normalized-to-area transmittance versus wavelength for a normal incident acoustic plane wave propagating in air and impinging in the grating. (c) Acoustic pressure distribution when extraordinary acoustic transmission occurs. (d) Details of the normalized-to-area transmittance when the wavelength is near 27 mm. (e) Details of the normalized-to-area-transmittance when the wavelength is near 59 mm.

length and width of the neck of the HRs were both 1 mm. The length and width of the cavity of the HRs were 6 and 5 mm, respectively. The lattice constant of the grating was 26 mm (each period covering four HRs and a narrow aperture). The blue line in Fig. 1(b) shows the calculated normalized-to-area transmittance versus wavelength for an incident acoustic planar wave impinging at the sample. A transmission peak can be found when the wavelength is 26.6 mm. This transmission peak is the same as that reported in Ref. [26] and results from the coupling between the diffractive waves excited on the surface and the Fabry-Perot resonant modes inside the apertures [28–31]. We also calculated the normalized-to-area transmittance of the grating sample without HRs, as shown by the red line in Fig. 1(b), and a transmission peak was also found at a wavelength of 26.9 mm. The occurrences of these two peaks are not surprising because their wavelengths are near the lattice constant of the grating (26 mm). Surprisingly, we found a transmission peak at a wavelength of 58.9 mm for the sample with HRs (blue line), and this wavelength was much larger than any characteristic length involved in the sample, such as the lattice constant of the grating (26 mm), the thickness of the grating (10 mm), and the period of the HRs (6 mm). But for the sample without HRs (red line), no other transmission peaks are found, so the extraordinary acoustic transmission for the sample with HRs cannot be attributed to the coupling between the diffractive waves and the Fabry-Perot resonant modes, which would be related to the width of the interlayer and the coherent diffraction of the periodic lattices. The enlarged normalized-to-area transmittances are also shown in Figs. 1(d) and 1(e) for details. Figure 1(c) presents the calculated acoustic pressure distributions at a wavelength of 58.9 mm. Strong surface waves are localized on the surface

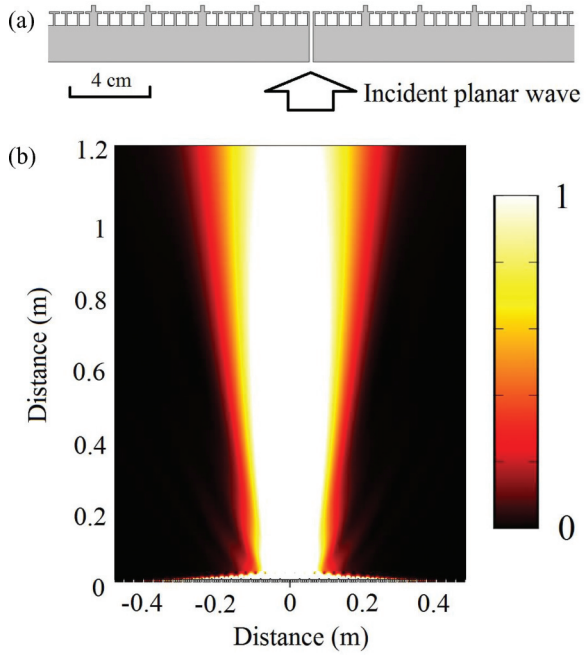

FIG. 2. (Color) (a) Schematic diagram of the structure to realize sound beam collimation when the transmission slit is much smaller than the wavelength. (b) Sound intensity distribution when collimation beam occurs.

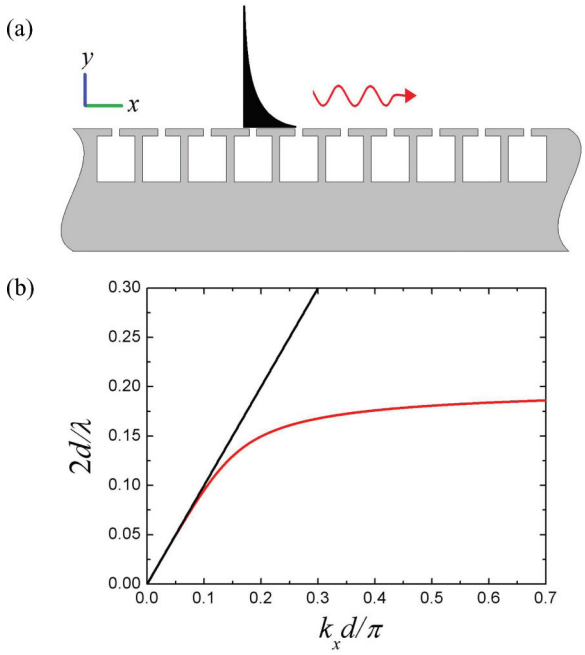

FIG. 3. (Color) (a) A series of periodic HRs cascaded together in order to excite acoustic collective surface oscillation. (b) Dispersion curve of the collective surface oscillation.

of the grating on the output side, similar to SPs at a metallic surface.

III. BEAMING SOUND

The system achieving acoustic beam collimation is a hard-plate-structured system consisting of a single slit surrounded by finite periodic two-dimensional HRs and rectangular gratings on the output side [Fig. 2(a)]. The lattice constant of the rectangular gratings is 27 mm. The length and the width of the rectangular gratings are 3 and 2 mm, respectively. The width of the center slit is 2 mm and the thickness of the plate is 25 mm. The parameters of the HRs are the same as those in Fig. 1(a). At a wavelength of 59.5 mm, a well-collimated beam is achieved, as shown in Fig. 2(b). The collimated beam reported in Refs. [32–34] is achieved when the wavelength is near the lattice constant of the gratings, and these collimated beams have strong side lobes. Different from previous works, the collimated beam reported herein was achieved when the wavelength was much larger than any characteristic length involved in the sample, and the collimated beam obtained is nearly without side lobes. Also, strong surface waves are localized on the surface of the plate on the output side [Fig. 2(b)].

IV. ACOUSTIC COLLECTIVE SURFACE OSCILLATIONS

Both of the above two structures induce strong acoustic surface waves on the surface of the plates on the output side. In this paragraph, we would like to find the mechanisms behind the extraordinary acoustic transmission and the collimation effect. The first question that needs to be answered is whether the strong acoustic surface waves are caused by the decorated two-dimensional HRs. In order to eliminate the influence of the period [i.e., periodic apertures in Fig. 1(a) or rectangular gratings in Fig. 2(a)], we would like to consider the acoustic surface waves caused by periodic two-dimensional HRs decorated on a rigid body [Fig. 3(a)]. On the subwavelength scale, the effective impedance of the boundary can be regarded as homogeneous and can be expressed as [38]

$$Z_s' = i\left(\frac{1}{\omega C_{\mathrm{HR}}} - \omega M_{\mathrm{HR}}\right)d, \tag{1}$$

where C_{HR} and M_{HR} are the acoustic capacitance and the acoustic mass of the two-dimensional HRs, respectively; d is the lattice constant of the HRs; $i = \sqrt{-1}$; and ω is the angular frequency. The resonance frequency of the HRs can be inferred as $\omega_{\mathrm{HR}} = \frac{1}{\sqrt{C_{\mathrm{HR}} M_{\mathrm{HR}}}}$. Assuming the acoustic pressure of the acoustic surface wave caused by the HRs to be

$$p = Ae^{-\gamma y}e^{i(k_x x - \omega t)}, \tag{2}$$

where x and y are Cartesian coordinates, t is time, A is the amplitude of the surface wave, k_x is the wave number in the x direction, and γ implies the decay of the surface wave along the y direction and satisfies

$$\gamma^2 = k_x^2 - \frac{\omega^2}{c_a^2}, \tag{3}$$

where c_a is the speed of the free space wave in air. According to the momentum conservation equation, $\frac{\partial p}{\partial y} - i\omega\rho_a v_y = 0$, we can obtain the expression of the particle velocity in the y direction.

$$v_y = \frac{i\gamma}{\omega\rho_a}Ae^{-\gamma y}e^{i(k_x x - \omega t)}, \tag{4}$$

where ρ_a is the air density. The relationship between the acoustic pressure (p) and normal particle velocity (v_n) at the boundary is governed by the effective impedance, given as

$$Z_s' = \left.\frac{p}{v_n}\right|_{y=0}. \tag{5}$$

Noticing $v_n = -v_y$ at the boundary ($y = 0$) and substituting Eqs. (1), (2), and (4) into Eq. (5), we obtain

$$\frac{i\omega\rho_a}{\gamma} = i\left(\frac{1}{\omega C_{\rm HR}} - \omega M_{\rm HR}\right)d. \tag{6}$$

This equation and Eq. (3) imply a dispersion relationship of the surface wave above the decorated rigid body,

$$k_x^2 c_a^2 = \omega^2 + \frac{1}{\left(\omega_{\rm HR}^2 - \omega^2\right)^2}\frac{(\rho_a c_a)^2\omega^4}{M_{\rm HR}^2 d^2}, \tag{7}$$

which is very similar to the typical SP dispersion relationship [39]. Figure 3(b) shows a sketch of the dispersion as a function of $k_x d/\pi$. It can be noticed that the surface mode approaches the light line asymptotically at low frequency, and the field associated with the mode expands into the free space. At large k_x, the frequency of the mode approaches $\omega_{\rm HR}$. Please note that very different from the acoustic surface wave caused by the grooves' structure [34], in our structure, the frequency to realize $k_x \to \infty$ is decreased a lot ($2d/\lambda \approx 0.17$), which can be utilized to realize device miniaturization.

To understand the collective surface oscillations caused by HRs, we first review the origin of SPs. The fact that metals support the collective oscillation of electrons bound to the surface is the result of free electrons that behave like a plasma with a dielectric function $\varepsilon = 1 - \frac{\omega_p^2}{\omega^2}$, which is negative below the plasma frequency, ω_p [1]. Free electrons and restoring forces are the two dominant factors. The oscillation of free electrons can be regarded as the oscillation of pistons near the equilibrium position. In acoustics, the air columns in the neck of the HRs can be regarded as the pistons that oscillate near the equilibrium position. The cavities of the HRs are responsible for providing the restoring forces, so the collective surface oscillations are realized in acoustics with a strong dispersion relation, which is almost the same as that of SPs when the frequency is below the resonance frequency of the HRs.

V. MECHANISM OF ACOUSTIC TRANSMISSION AND COLLIMATION

To understand the mechanism of extraordinary acoustic transmission realized by the acoustic grating with HRs [Fig. 1(a)], we first repeat the mechanism of extraordinary acoustic transmission realized by the acoustic grating without HRs [26]: When the wavelength is near the period of the rectangular acoustic grating, evanescent high-order modes are greatly excited, which induces an additional acoustical reactance. This reactance greatly changes the effective thickness of the grating, which results in extraordinary acoustic transmission [30,31]. However, because their acoustic grating is without HRs, high-order modes cannot be excited when the wavelength is much larger than the period of the grating. So extraordinary acoustic transmission cannot be achieved at very low frequency. In our structure, the two-dimensional HRs can stimulate collective surface oscillations on the surface of the plate on the output side when the wavelength is much larger than the period of the grating, which acts as high-order modes, so we can understand why the extraordinary acoustic transmission phenomenon can be achieved.

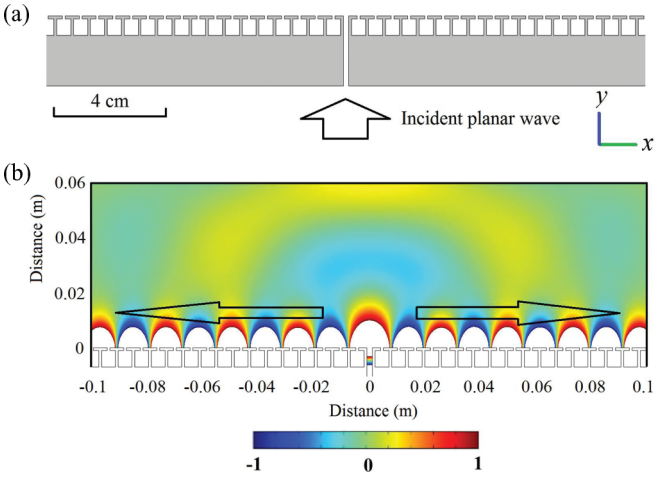

FIG. 4. (Color) (a) A hard plate consists of a single slit surrounded by finite periodically two-dimensional HRs. (b) Acoustic pressure distribution in the output side of the plate when the frequency is below the resonance frequency of the HRs. Here, the frequency is 5762 Hz.

In order to find the mechanism of the sound beam collimation effect, we should consider the factors of the periodic HRs and the rectangular gratings in the hard-plate-structured system [Fig. 2(a)], separately. First, we would like to remove the rectangular gratings of the system and retain the periodic HRs and the single slit of the system. The sample is shown in Fig. 4(a). The thickness of the plate, the width of the center slit, and the parameters of the HRs are the same as those in Fig. 2(a). A normal incident acoustic plane wave propagates in air and impinges at the single slit. After traveling through the plate, the incident acoustic wave strongly couples into the collective surface oscillations and travels along the surface of the plate in the output side, as shown in Fig. 4(b). Owing to the fact that the width of the slit is much smaller than the wavelength, the output side of the slit can be considered as a point source. Its Green's function is [38]

$$G(x,y) = \frac{i}{4\pi}\int_{-\infty}^{\infty}\frac{k_y Z_s'}{k_y Z' + \omega\rho_a}\frac{e^{i(k_x x + k_y|y|)}}{k_y}dk_x. \tag{8}$$

Here, k_x and k_y are the wave-vector components in the x and y directions, respectively, satisfying $k_y = i\sqrt{k_x^2 - k^2}$, where k is the wave number in air. For a point source in infinite space, its plane-wave expansion form is

$$G(x,y) = \frac{i}{4\pi}\int_{-\infty}^{\infty}\frac{e^{i(k_x x + k_y|y|)}}{k_y}dk_x. \tag{9}$$

Compared with Eq. (9), Eq. (8) is multiplied by one more factor, $\frac{k_y Z'}{k_y Z_s' + \omega\rho_a}$. This factor tailors the scale of each k_x owing to the introduction of HRs. This factor turns out to be infinitely

large when

$$k_y Z_s' + \omega \rho_\alpha = 0. \tag{10}$$

This mode (k_x) is the main mode for the wave transmitting through the plate. Notice the effective impedance of the surface of the plate in the output side is $Z_s' = i(\frac{1}{\omega C_{\rm HR}} - \omega M_{\rm HR})d$. Substituting the formula into Eq. (10), we obtain the dispersion relationship of the main traveling mode in the output side of the plate:

$$k_x^2 c_a^2 = \omega^2 + \frac{1}{\left(\omega_{\rm HR}^2 - \omega^2\right)^2} \frac{(\rho_a c_a)^2 \omega^4}{M_{\rm HR}^2 d^2}. \tag{11}$$

This is the same as Eq. (7), which implies that the main traveling mode on the output side of the plate is the collective surface oscillations. This can be regarded as a method to stimulate acoustic collective surface oscillations, which corresponds to the near-field excitation of SPs in optics [40].

The rectangular gratings act as antennae to couple the collective surface oscillations to a radiation wave at a specific wavelength, which results in the collimation effect. The matching condition in the x direction is $k_{\rm out} \sin\theta = k_{\rm CSO} \pm nG$, where θ is the transmitting angle; $k_{\rm CSO}$ and G are the momentum of the collective surface oscillations caused by HRs and the momentum of the rectangular gratings, respectively. When $k_{\rm CSO} = nG$ which implies the transmitting angle $\theta = 0$, the collimation beam is realized.

VI. DISCUSSION

To verify the existence of the acoustic collective surface oscillations, we constructed a rigid plate decorated with periodic two-dimensional HRs. The period of the HRs was 6 mm. The parameters of the HRs are the same as those in Fig. 1(a). Because the dispersion curve of the collective surface oscillations is always located at the right side of the light line and the wave vector of the collective surface oscillations is larger than the wave vector in air, the collective surface oscillations cannot be stimulated by an illuminating plane wave on the decorated plate with any incident angle. In optics, optical gratings are used to couple the incident wave into the surface mode and stimulate SPs [41]. Inspired by this approach, we used acoustic gratings to stimulate collective surface oscillations. Eight rectangular gratings were introduced to the left side of the surface of the decorated plate, as shown in Fig. 5(a). The lattice constant of the rectangular gratings was 36 mm, therefore covering six HRs in each period. The length and width of the gratings were 4 and 2 mm, respectively. The details of the decorated plate and the rectangular gratings are also shown in Fig. 5(a). The introduction of the rectangular gratings corresponds to adding

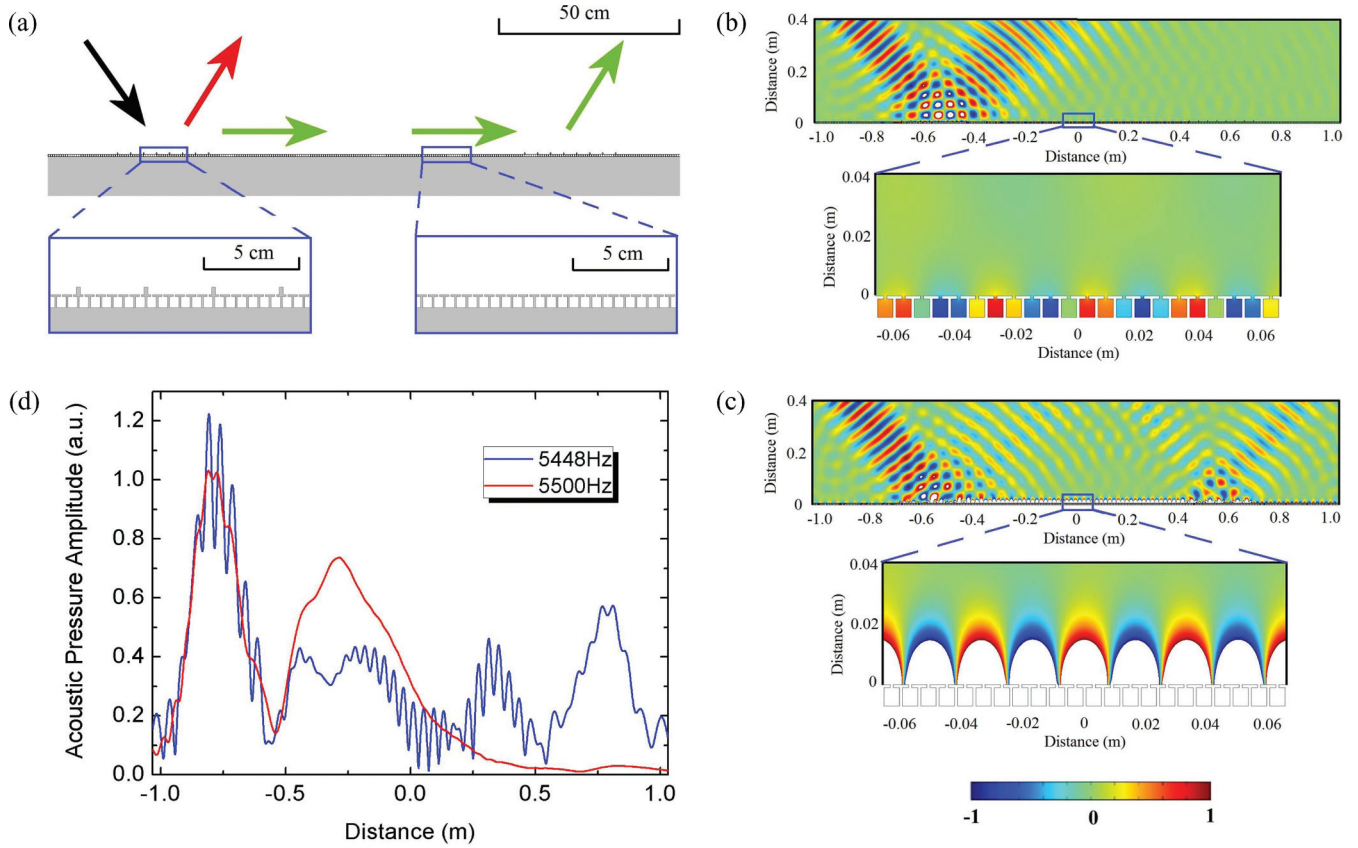

FIG. 5. (Color) (a) Schematic diagram of the structure to excite and detect the collective surface oscillation. The structure is a rigid plate decorated with periodic HRs on its surface and several rectangular gratings on both sides. (b) Acoustic pressure distribution when matching condition is not satisfied. Here the frequency is 5500 Hz. (c) Acoustic pressure distribution when matching condition is satisfied. Here the frequency is 5448 Hz. (d) Acoustic pressure amplitude distribution at $y = 0.3$ m when the matching condition is satisfied.

extra momentum to the incident wave. For an incident wave with wave vector k_i and incident angle θ. If the matching condition, $k_i \sin\theta + nG = k_x$, is satisfied then the incident wave can be greatly coupled into surface modes and the collective surface oscillation is stimulated. Here, G is the amplitude of the introduced reciprocal lattice vector induced by the rectangular gratings and n is an integer. Otherwise, the incident wave is reflected according to the reflection law. Since there are no fluorescent molecules in acoustics, the best way to detect the collective surface oscillation is to scatter it and radiate the surface wave to the far field. We introduced eight rectangular gratings to the right side of the surface of the decorated plate, as shown in Fig. 5(a). Reversed progress will take place to couple the collective surface oscillation into a radiation wave when the matching condition, $k_r \sin\theta = k_x - nG$, is satisfied. Here, k_r is the wave vector of the radiation wave. In Fig. 5(a), the black arrow indicates the incident acoustic wave. If the matching condition is not satisfied, the incident wave is reflected as shown by the red arrow. When the matching condition is satisfied, the incident wave is largely coupled into the collective surface oscillation and travels along the surface of the plate before meeting the rectangular gratings on the right side, as shown by the green horizontal arrow. When the traveling collective surface oscillation meets the rectangular gratings on the right side, it will be coupled into the radiation wave, which can be detected at the far field, as shown by the green slanted arrow. Figure 5(b) presents the simulation results when the matching condition is not satisfied. The frequency here is 5500 Hz (the wavelength is 62.4 mm) and the incident angle is 40°. The incident and reflected wave meet the reflection law and no collective surface oscillation is stimulated. When the frequency is 5448 Hz (the wavelength is 63.0 mm), however, the reflected wave is greatly decreased, as shown in Fig. 5(c). It is obvious that a strong collective surface oscillation is stimulated and that it is well confined on the surface of the plate. When the traveling collective surface oscillation meets the right rectangular gratings, it is radiated to the far field. If we regard the radiation wave caused by the right rectangular gratings as another kind of reflected wave, then in this situation, the incidence point and the reflection point maintain their distance. It is worth noticing that this distance is arbitrary. Figure 5(d) presents the acoustic pressure amplitude at $y = 0.3$ m. For the 5500-Hz incident wave, the profiles of the incident wave and the reflected wave are close. But for the 5448-Hz incident wave, the profiles of the incident wave and the reflected wave keep a long distance because of the stimulation of the collective surface oscillation.

VII. CONCLUSION

In conclusion, we have proposed two acoustic examples of the collective surface oscillation on the surface of hard plates, mimicking SPs in the optical case. Unlike well-known acoustic surface waves such as Rayleigh waves and structure-induced acoustic surface waves, the imitation SPs in acoustics are closely analogous to SPs in optics in that they show almost the same dispersion curve at low frequency. The surface collective oscillations found in this study can anticipate many exotic acoustical phenomena, similar to those found in the optical case related to SPs.

ACKNOWLEDGMENTS

We acknowledge the National Basic Research Program of China (Grants No. 2012CB921504 and No. 2011CB707902); financial support of the National Natural Science Foundation of China (Grant No. 11474160); fundamental research funds for the Central Universities (No. 020414380001); State Key Laboratory of Acoustics, Chinese Academy of Science (Grant No. SKLOA201401); the priority academic program development of Jiangsu Higher Education Institutions; and SRF for ROCS and SEM.

[1] R. H. Ritchie, Plasma losses by fast electrons in thin films, Phys. Rev. **106**, 874 (1957).
[2] N. Yu, P. Genevet, M. A. Kats, F. Aieta, J. P. Tetienne, F. Capasso, and Z. Gaburro, Light propagation with phase discontinuities: Generalized laws of reflection and refraction, Science **334**, 333 (2011).
[3] A. Silva, F. Monticone, G. Castaldi, V. Galdi, A. Alu, and N. Engheta, Performing mathematical operations with metamaterials, Science **343**, 160 (2014).
[4] D. Erickson, X. Serey, Y. F. Chen, and S Mandal, Nanomanipulation using near field photonics, Lab Chip **11**, 995 (2011).
[5] M. C. Zhong, X. B. Wei, J. H. Zhou, Z. Q. Wang, and Y. M. Li, Trapping red blood cells in living animals using optical tweezers, Nat. Commun. **4**, 1768 (2013).
[6] A. Arbouet, N. Del Fatti, and F Valle, Optical control of the coherent acoustic vibration of metal nanoparticles, J. Chem. Phys. **124**, 144701 (2006).
[7] M. L. Juan, M. Righini, and R. Quidant, Plasmon nano-optical tweezers, Nat. Photon. **5**, 349 (2011).
[8] D. Brinks, F. D. Stefani, F. Kulzer, R. Hildner, T. H. Taminiau, Y. Avlasevich, K. Müllen, and N. F. van Hulst, Visualizing and controlling vibrational wave packets of single molecules, Nature **465**, 905 (2010).
[9] S. Nie and S. R. Emory, Probing single molecules and single nanoparticles by surface-enhanced Raman scattering, Science **275**, 1102 (1997).
[10] V. J. Sorger and X Zhang, Spotlight on plasmon lasers, Science **333**, 709 (2011).
[11] K. Kneipp, H. Kneipp, I. Itzkan, R. R. Dasari, and M. S. Feld, Surface enhanced Raman scattering and biophysics, J. Phys.: Condens. Matter **14**, R597 (2002).
[12] J. Bravo-Abad, F. J. Garci-Vidal, and L Martin-Moreno, Resonant Transmission of Light through Finite Chains of Subwavelength Holes in a Metallic Film, Phys. Rev. Lett. **93**, 227401 (2005).
[13] H. F. Fhaemi, T. Thio, D. E. Grupp, T. W. Ebbesen, and H. J. Lezec, Surface plasmons enhance optical transmission through subwavelength holes, Phys. Rev. B **58**, 6779 (1998).

[14] T. W. Ebbesen, H. J. Lezec, H. F. Ghaemi, T. Thio, and P. A. Wolff, Extraordinary optical transmission through sub-wavelength hole arrays, Nature **391**, 667 (1998).
[15] H. J. Lezec, A. Degiron, E. Devaux, R. A. Linke, L. Martin-Moreno, F. J. Garcia-Vidal, and T. W. Ebbesen, Beaming light from a subwavelength aperture, Science **297**, 820 (2002).
[16] P. Berini and I. De Leon, Surface plasmon-polariton amplifiers and lasers, Nat. Photon. **6**, 16 (2011).
[17] F. van Beijnum, P. J. van Veldhoven, E. J. Geluk, and M. J. A. de Dood, Surface Plasmon Lasing Observed in Metal Hole Arrays, Phys. Rev. Lett. **110**, 206802 (2013).
[18] A. Minovich, A. E. Klein, N. Janunts, T. Pertsch, D. N. Neshev, and Y. S. Kivshar, Generation and Near-Field Imaging of Airy Surface Plasmons, Phys. Rev. Lett. **107**, 116802 (2011).
[19] L. Li, T. Li, S. M. Wang, and S. N. Zhu, Collimated Plasmon Beam: Nondiffracting versus Linearly Focused, Phys. Rev. Lett. **110**, 046807 (2013).
[20] M. S. Tame, K. R. McEnery, Ş. K. Özdemir, J. Lee, S. A. Maier, and M. S. Kim, Quantum plasmonics, Nat. Phys. **9**, 329 (2013).
[21] K. O'Brien, N. D. Lanzillotti-Kimura, J. Rho, H. Suchowski, X. Yin, and X. Zhang, Ultrafast acousto-plasmonic control and sensing in complex nanostructures, Nat. Commun. **5**, 4042 (2014).
[22] W. L. Barnes, W. A. Murray, J. Dintinger, E. Devaux, and T. W. Ebbesen, Surface Plasmon Polaritons and Their Role in the Enhanced Transmission of Light through Periodic Arrays of Subwavelength Holes in a Metal Film, Phys. Rev. Lett. **92**, 107401 (2004).
[23] Q. Cao and P Lalanne, Negative Role of Surface Plasmons in the Transmission of Metallic Gratings with Very Narrow Slits, Phys. Rev. Lett. **88**, 057403 (2002).
[24] X Zhang, Acoustic resonant transmission through acoustic gratings with very narrow slits: Multiple-scattering numerical simulations, Phys. Rev. B **71**, 241102 (2005).
[25] B. Hou, J. Mei, M. Ke, W. Wen, Z. Liu, J. Shi, and P. Sheng, Tuning Fabry-Perot resonances via diffraction evanescent waves, Phys. Rev. B **76**, 054303 (2007).
[26] M.-H. Lu, X.-K. Liu, L. Feng, J. Li, C.-P. Huang, Y.-F. Chen, Y.-Y. Zhu, S.-N. Zhu, and N.-B. Ming, Extraordinary Acoustic Transmission through a 1D Grating with Very Narrow Apertures, Phys. Rev. Lett. **99**, 174301 (2007).
[27] L. Zhou and G. A. Kriegsmann, Complete transmission through a periodically perforated rigid slab, J. Acoust. Soc. Am. **121**, 3288 (2007).
[28] J. Christensen, L. Martin-Moreno, and F. J. Garcia-Vidal, Theroy of Resonant Acoustic Transmission through Subwavelength Apertures, Phys. Rev. Lett. **101**, 014301 (2008).
[29] H. Estrada, P. Candelas, A. Uris, F. Belmar, F. J. García de Abajo, and F. Meseguer, Extraordinary Sound Screening in Perforated Plates, Phys. Rev. Lett. **101**, 084302 (2008).
[30] X. Wang, Acoustical mechanism for the extraordinary sound transmission through subwavelength apertures, Appl. Phys. Lett. **96**, 134104 (2010).
[31] X. Wang, Theory of resonant sound transmission through small apertures on periodically performated slabs, J. Appl. Phys. **108**, 064903 (2010).
[32] J. Christensen, A. I. Fernandez-Dominguez, F. de Leon-Perez, L. Martin-Moreno, and F. J. Garcia-Vidal, Collimation of sound assisted by acoustic surface waves, Nat. Phys. **3**, 851 (2007).
[33] Y. Zhou, M.-H. Lu, L. Feng, X. Ni, Y.-F. Chen, Y.-Y. Zhu, S.-N. Zhu, and N.-B. Ming, Acoustic Surface Evanescent Wave and Its Dominant Contribution to Extraordinary Acoustic Transmission and Collimation of Sound, Phys. Rev. Lett. **104**, 164301 (2010).
[34] J. Christensen, L. Martin-Moreno, and F. J. Garcia-Vidal, Enhanced acoustical transmission and beaming effect through a single aperture, Phys. Rev. B **81**, 174104 (2010).
[35] L. Kelders, J. F. Allard, and W Lauriks, Ultrasonic surface waves above rectangular-groove gratings, J. Acoust. Soc. Am. **103**, 2730 (1998).
[36] H. Jia, M. Lu, Q. Wang, M. Bao, and X. Li, Subwavelength imaging through spoof surface acoustic waves on a two-dimensional structured rigid surface, Appl. Phys. Lett. **103**, 103505 (2013).
[37] Y. Ye, M. Ke, Y. Li, T. Wang, and Z. Liu, Focusing of spoof surface-acoustic-waves by a gradient-index structure, J. Appl. Phys. **114**, 154504 (2013).
[38] L. Quan, X. Zhong, X. Liu, X. Gong, and P. A. Johnson, Effective impedance boundary optimization and its contribution to dipole radiation and radiation pattern control, Nat. Commun. **5**, 3188 (2014).
[39] J. B. Pendry, L. Martin-Moreno, and F. J. Garcia-Vidal, Mimicking surface plasmons with structured surfaces, Science **305**, 847 (2004).
[40] B. Hecht, H. Bielefeldt, L. Novotny, Y. Inouye, and D. W. Pohl, Local Excitation, Scattering, and Interference of Surface Plasmons, Phys. Rev. Lett. **77**, 1889 (1996).
[41] I. R. Hooper and J. R. Sambles, Dispersion of surface plasmon polaritons on short-pitch metal gratings, Phys. Rev. B **65**, 165432 (2002).